IET Nanobiotechnology

Research Article

IET Journals
The Institution of Engineering and Technology

Antibacterial and catalytic activity of biogenic gold nanoparticles synthesised by *Trichoderma harzianum*

ISSN 1751-8741
Received on 30th April 2017
Revised 8th December 2017
Accepted on 30th December 2017
E-First on 20th March 2018
doi: 10.1049/iet-nbt.2017.0105
www.ietdl.org

Ravi Mani Tripathi[1], Braj Raj Shrivastav[2], Archana Shrivastav[3] ✉

[1]*Amity Institute of Nanotechnology, Amity University, Sector 125, Noida 201303, India*
[2]*Department of Surgical Oncology, Cancer Hospital & Research Institute, Gwalior 474009, Madhya Pradesh, India*
[3]*Department of Microbiology, College of Life Sciences, Gwalior 474009, Madhya Pradesh, India*
✉ *E-mail: archanashrivastav.chri@gmail.com*

Abstract: This study reveals the antibacterial and catalytic activity of biogenic gold nanoparicles (AuNPs) synthesised by biomass of *Trichoderma harzianum*. The antibacterial activity of AuNPs was analysed by the means of growth curve, well diffusion and colony forming unit (CFU) count methods. The minimum inhibitory concentration of AuNPs was 20 µg/ml. AuNPs at 60 µg/ml show effective antibacterial activity as optical absorption was insignificant. The well diffusion and CFU methods were also applied to analyse the effect of various concentration of AuNPs. Further, the catalytic activity of AuNPs was analysed against methylene blue (MB) as a model pollutant in water. MB was degraded 39% in 30 min in the presence of AuNPs and sodium borohydrate and the rate constant (k) was found to be 0.2×10^{-3} s^{-1}. This shows that the biogenic AuNP is an effective candidate for antibacterial and catalytic degradation of toxic pollutants.

1 Introduction

Gold nanoparticles (AuNPs) have gained attention of researchers due to their applications in various fields such as optoelectronic, electronic and magnetic devices, and catalysts, sensors and drug delivery. These applications are mainly depending on shape, size, crystallinity and structure [1]. The various shapes of gold nanostructures have been reported like nanocubes [2], nanowires [3], nanoplates [4], nanospheres [5], nanorods [6], nanopoles [7], nanobelts [8] and unusual angled shapes [9]. One-dimensional (1D) metallic nanostructures have long been of consideration to many groups of researchers [10]. AuNPs have attracted the researchers due to their unique and tunable surface plasmon resonance. AuNPs have also gained importance in biomedical application than the other metallic nanostructures because of their non-cytotoxicity and biocompatibility [11]. AuNPs can be synthesised easily with high chemical and thermal stability [12]. AuNPs were utilised as detection tools in molecular imaging using fluorescence resonance energy transfer due to their unique biocompatibility and well-defined surface chemistry [13–15].

Metallic nanomaterials are massive and growing area because of their potential application in various fields such as healthcare, agriculture, environment and energy [16–19]. The chemical method of nanomaterials synthesis is expensive and cause serious environmental problems. Nowadays, researchers are using biological methods for synthesis of nanomaterials using plants extract [16, 20–22], fungal biomass [23–25] and bacterial biomass [26, 27]. These synthesis methods offer advantages over existing synthetic method due to its eco-friendliness and also eradicates the toxicity-related concerns making these materials to be used for a wide variety of biological applications [16].

Organic dyes are widely used in several industries such as in textile, food, cosmetics, leather, paper and plastic industries. These dyes are highly toxic to biological systems and cause serious environmental effect. These dyes are not degrading in environment as it is highly chemically and thermo-stable and resistant to biodegradation. Heterocyclic aromatic azo dyes such as methylene blue (MB) are used in paint production and textile industries. Methylene blue is a monoamine oxidase inhibitor [28] and cause severe serotonin toxicity upon intravenous infusion [29].

The conventional processes such as precipitation, flocculation, flotation, adsorption, oxidation, reduction, electrochemical, aerobic, anaerobic and biological treatment methods are not adequate for completely degradation of dyes. These processes have inbuilt limitations like less efficiency and production of secondary sludge, and the removal of sludge is an expensive concern [30–32]. A number of processes have been applied for the wastewater treatment such as coagulation, flocculation, adsorption, membrane filtration, biological treatment, electrochemical, ion exchange and chemical oxidation [33, 34]. Chemical coagulation is required huge amount of chemical [35]. The flocculation process for wastewater treatment is cost effective and utilises less energy [36]. Although chemicals applied such as aluminium chloride and aluminium sulphate in coagulation and flocculation have become controversial due to the possibility to cause Alzheimer's disease [35, 36]. Adsorption method for wastewater treatment is simple and effective but it generally produces huge amount of sludge, especially in the wastewater with high dye concentrations [37]. The activated carbon has been found a prominent material for effective catalyst because of its high specific surface area, high adsorption capacity, and low selectivity for non-ionic and ionic dyes. Whereas these materials are costly, need of regeneration after use and loses adsorption efficiency of regenerated activated carbon [37]. Nowadays, metal/metal oxide nanostrucures are extensively used for catalytic/photocatalytic activity.

AuNPs were synthesised by biological method using biomass of *Trichoderma harzianum*. The antibacterial activity of AuNPs was evaluated by growth curve, well diffusion and colony forming unit (CFU) methods against *Escherichia coli*. Catalytic activity of AuNPs was also analysed against MB as a model pollutant.

2 Materials and methods

2.1 Materials

The fungal strain of *T. harzianum* was obtained from Department of Microbiology, College of Life Sciences, Gwalior, India. Luria Bertani media were supplied by Hi-Media Laboratories, Bombay, India. Potato dextrose agar, malt extract, yeast extract, peptone and glucose were purchased from Hi-media, Mumbai, India. Chloroauric acid, MB and sodium borohydrate ($NaBH_4$) were purchased from Qualigens Fine Chemicals, Mumbai, India.

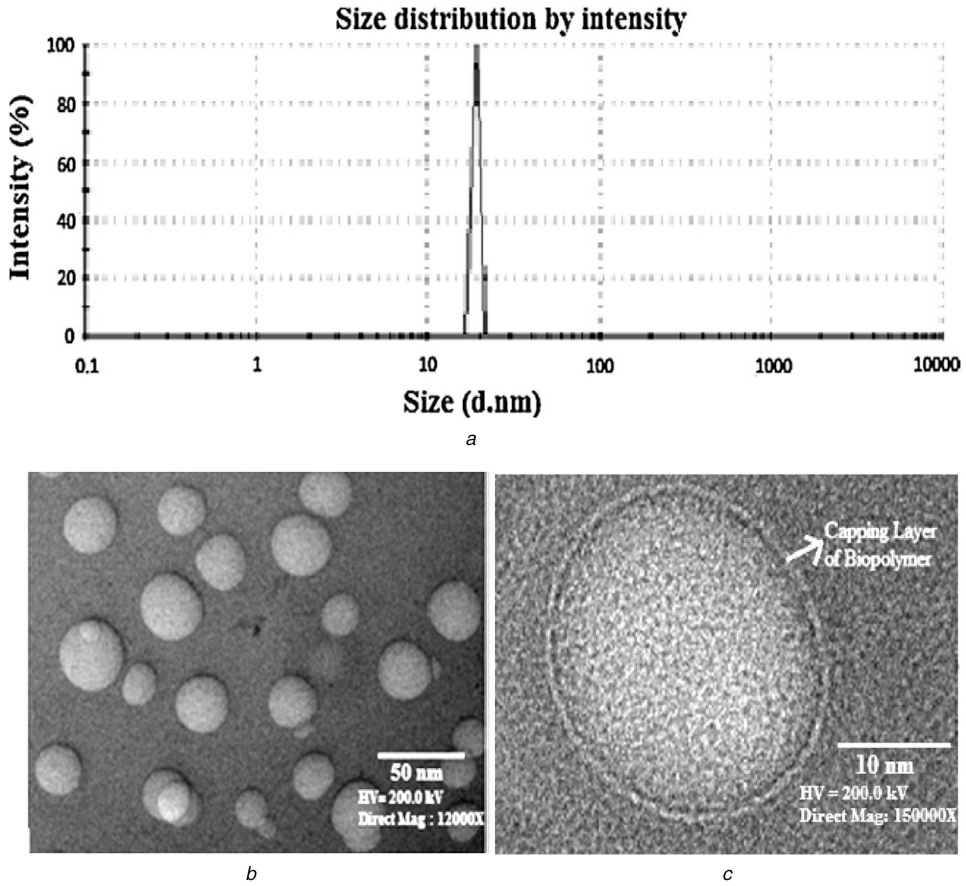

Fig. 1 *Biosynthesised gold nanoparticles using biomass of T. harzianum*

(a) DLS showing size distribution profile of biosynthesised AuNPs, ***(b)*** TEM micrograph showing AuNPs synthesised by *T. harzianum*, ***(c)*** TEM micrograph at high-resolution showing single nanoparticles with clear capping layer. Figures are reproduced from Tripathi *et al.* [23], with the permission of Elsevier Science

2.2 Biosynthesis of AuNPs

AuNPs were synthesised using biological method developed by Tripathi *et al.* [23]. Briefly, *T. harzianum* was inoculated in 100 ml MYPG medium (malt extract 0.3%, yeast extract 0.3%, peptone 0.3% and glucose 1%) for preparation of biomass. Culture was incubated in the dark condition at 28 ± 1°C for 120h. Finally, the biomass was extracted from the media and washed with deionised water. The fungal biomass (5 g) was dispersed into deionised water and adds 1 mM chloroauric acid. The mixture was then kept at 28 ± 1°C in dark condition with continuous shaking at 200 rpm for 72 h. After 72 h of incubation, AuNPs were separated and purified from mixture solution (Fig. 1). The size distribution profile of biosynthesised AuNPs was analysed by dynamic light scattering (DLS). Transmission electron microscopy (TEM) was used to analyse the size and morphology of the synthesised AuNPs. The carbon-coated copper grid was used to prepare thin film of sample for analysis.

2.3 Evaluation of antibacterial activity

E. coli MTCC 1302 strain selected for the study to analyse the antibacterial nature of biosynthesised AuNPs. The reason behind the selection of *E. coli* MTCC 1302 is easy to culture, quick doubling time and easy in culture maintain. *E. coli* cannot sporulate as it is Gram-negative bacteria. The antibacterial activity of AuNPs was analysed by the means of growth curve, well diffusion and CFU count method.

2.3.1 Growth curve: Bacterial growth dynamics can be studied by plotting the cell growth (absorbance) versus the incubation time or log of cell number versus time. The obtained curve is known as growth curve. The broth media was supplemented with AuNPs (20–60 µg/ml) and the fresh colonies were inoculated from agar media and incubated at 37°C for 24 h with continuous shaking at 200 rpm. The growth of *E. coli* MTCC 1302 in broth media was indexed by measuring the optical density (at $\lambda = 600$ nm) at regular intervals using UV–vis spectrophotometer. The control culture was treated with similar fashion but without exposure of AuNPs.

2.3.2 Well diffusion: The antibacterial activity of biosynthesised nanoparticles was also assayed by the means of well-diffusion method. Petri-plates were prepared with Luria Bertani (LB) agar media. The well was created on LB agar media having 8 mm diameter and bacteria culture was spread on it. AuNPs were loaded with 4, 6 and 12 µg concentrations in the wells. The control well was also treated with similar fashion but without exposure of AuNPs. The plates were incubated at 37°C for 24 h and the inhibition zones were measured.

2.3.3 Colony forming unit: Bacterial colony counting is a convincing technique for the analysis of antibacterial activity of nanoparticles. Antibacterial activity of the AuNPs was further analysed by measuring the number of colonies grown. The LB agar media was supplemented with AuNPs ranging from 20 to 60 µg/ml. *E. coli* MTCC 1302 was culture on the media and incubate for 24 h at 37°C. The control culture was also treated with similar fashion but without exposure of AuNPs.

2.4 Catalytic activity

The catalytic activity of biosynthesised AuNPs was investigated using model dye MB. UV–vis spectroscopy was used in order to measure the absorbance. The catalytic activity of AuNPs was investigated by taking the absorbance values of reaction mixtures. The freshly prepared 1.0 ml aqueous solution of $NaBH_4$ (15 mM), 1.5 ml M.B (0.2 mM) and 0.25 ml biosynthesised AuNPs were mixed in the standard quartz cuvette having 1 cm path length. The absorption spectra were recorded by UV–Vis spectroscopy with scanning range of 400–700 nm.

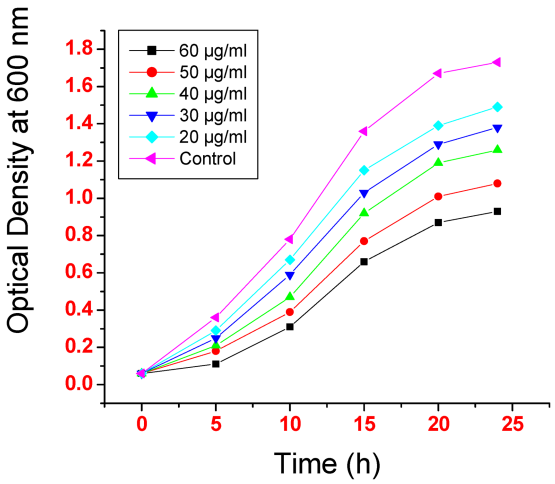

Fig. 2 *Effect of various concentrations of biosynthesised AuNPs on E. coli MTCC 1302 growth rate*

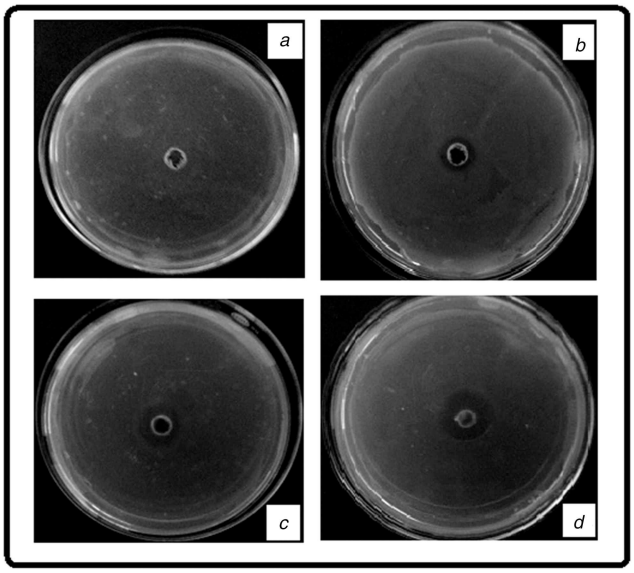

Fig. 3 *Photograph images of the inhibition zones (mm) observed with bacterial strain culture (E. coli MTCC 1302) plates loaded with AuNPs having*
(a) 0 µg, ***(b)*** 4 µg, ***(c)*** 6 µg, ***(d)*** 12 µg concentrations

3 Results and discussions

3.1 Biosynthesised AuNPs

DLS was used to analysed size distribution profile of biosynthesised AuNPs and found in the range of 32–44 nm in diameter (Fig. 1*a*). This shows that fungal biomass is supporting the synthesis of narrow size range of nanoparticles. TEM micrograph reveals that biogenic AuNPs are having particles size in the range of 26–34 nm (Fig. 1*b*) with spherical morphology. Fig. 1*c* shows clear layer of biopolymer as capping layer on nanoparticles which comes from fungal biomass [23].

3.2 Analysis of antibacterial of AuNPs

3.2.1 Growth curve analysis: The growth rate of *E. coli* MTCC 1302 was studied in the presence of biosynthesised AuNPs to evaluate their antibacterial activity. The optical densities were measured and plotted as a function of time for 24 h at regular intervals in the presence of various concentrations of AuNPs ranging from 20 to 60 µg/ml. It was scrutinised that optical densities of bacteria diminish with increase in the concentration of AuNPs (Fig. 2). It was observed that in the absence of AuNPs, there is increase in the optical density indicating bacterial growth but as the AuNPs concentration increases optical density decreases showing reduction of bacterial growth and shows no growth at 60 µg/ml as optical absorption was insignificant. The minimum inhibitory concentration (MIC) of AuNPs was 20 µg/ml (Fig. 2).

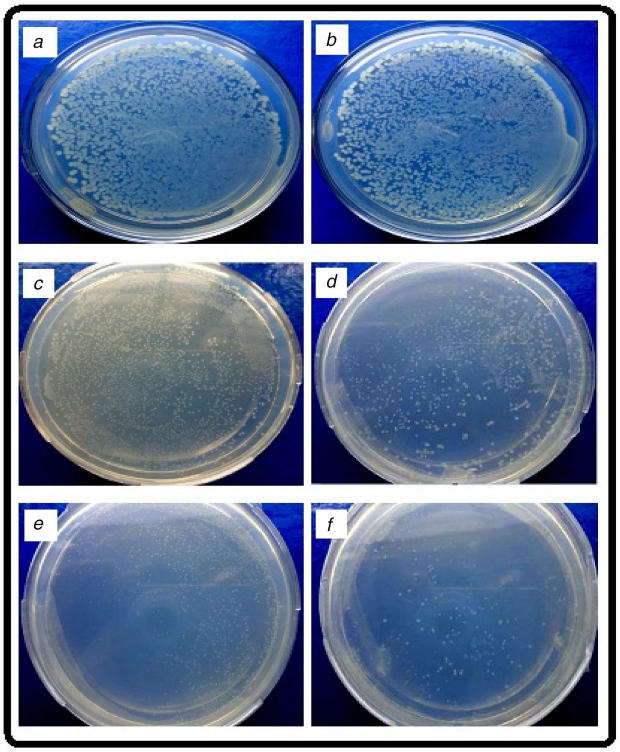

Fig. 4 *Photograph images of the number of colonies observed with bacterial strain culture (E. coli MTCC 1302) plates media supplemented with AuNPs having*
(a) 0 µg/ml, ***(b)*** 20 µg/ml, ***(c)*** 30 µg/ml, ***(d)*** 40 µg/ml, ***(e)*** 50 µg/ml, ***(f)*** 60 µg/ml concentrations

3.2.2 Well-diffusion analysis: The well-diffusion experiment was another technique for evaluation of antibacterial activity by measuring the diameter of zone. In our experiment it was found that the diameter of zone increases with increasing concentration of AuNPs. The inhibition zone was not observed in case of control (without any exposure of AuNPs). The diameter of zones was found to be 3, 5 and 9 mm with 4, 6 and 12 µg concentrations of AuNPs, respectively. The experimental results indicated that the AuNPs show effective antibacterial activity (Fig. 3).

3.2.3 CFU analysis: The antibacterial activity of AuNPs was also analysed by the means of CFU. AuNPs were supplemented with LB agar media ranging from 20 to 60 µg/ml. After 24 h of incubation of culture, dissimilar numbers of colonies were observed on the surface of media (Fig. 4). The maximum number of colonies was recorded in case of control culture and number colonies decreasing with increasing concentration of AuNPs. CFU graph shows that the 60 µg/ml concentration of AuNPs having effective antibacterial activity.

Further, antibacterial activity of nanoparticles was represented by plotted a graph between viable colony number and the concentration of AuNPs (Fig. 5). The graph clearly indicates that the number of colonies decreases with the increasing concentration of nanoparticles.

3.3 Catalytic activity of AuNPs

The catalytic reduction of MB by biogenic AuNPs was investigated. The reduction of MB in the presence of $NaBH_4$ was analysed and found no visible outcome in the absence of nanoparticles. The rapid reduction of MB was observed after addition of AuNPs. UV–vis absorption spectra of the reduction of MB by $NaBH_4$ in the presence of AuNPs recorded in 10 min intervals for a period of 30 min (Fig. 6). The absorbance peak occurred at 664 nm and showed remarkable decrease in the

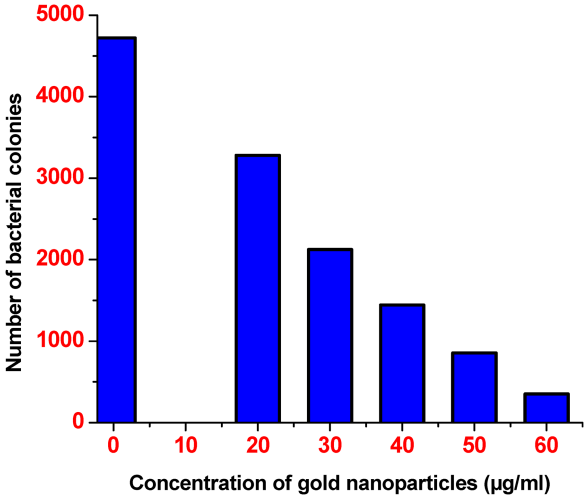

Fig. 5 *Graph shows the effect of AuNPs on the number of colonies grown on the LB media containing different concentrations of AuNPs*

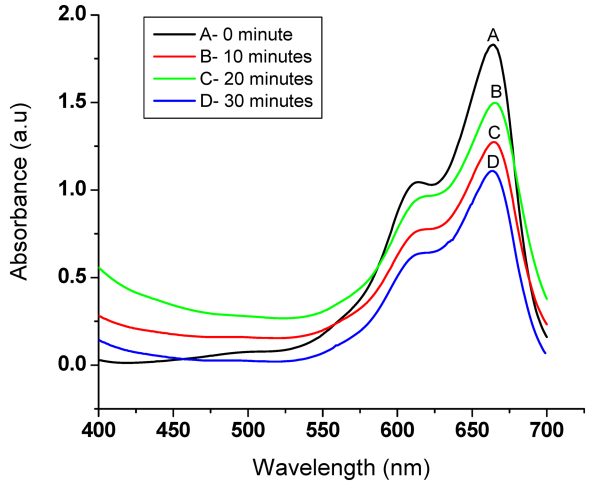

Fig. 6 *UV–vis spectra of the reduction of MB: 0.2 mM MB with 15 mM $NaBH_4$ in the presence of the as-prepared AuNPs as catalyst*

absorbance. After 30 min, 39% reduction of MB was observed in presence of AuNPs.

The MB concentration is fewer than the $NaBH_4$ in reduction process which causes the complete reduction of MB and the concentration of BH_4^- remains constant throughout the reaction. Therefore, catalytic activity of the AuNPs can be determined by the pseudo-first-order kinetics with respect to MB [38]. The rate constant (k) was determined from the linear plot of ln (A_t/A_0) versus reduction time in seconds which was estimated to be 0.2×10^{-3} s^{-1} (Fig. 7).

4 Conclusions

In the present study, we have investigated the antibacterial and catalytic activity of AuNPs. The antibacterial activity of AuNPs was evaluated by the means of growth curve, well diffusion and CFU counts methods. The various concentrations of AuNPs were used and found very small quantity of nanoparticles show effective antibacterial activity. The MIC of AuNPs was found to be 20 µg/ml against *E. coli* MTCC 1305. The biogenic AuNPs were also showing effective catalytic reduction of MB as 39% reduction was observed in 30 min. The rate constant (k) was estimated to be 0.2×10^{-3} s^{-1}. We can conclude that the AuNPs have good catalytic and antibacterial activity.

5 Acknowledgment

RMT thanks to the Amity University, Noida, India for providing an excellent facility for this work.

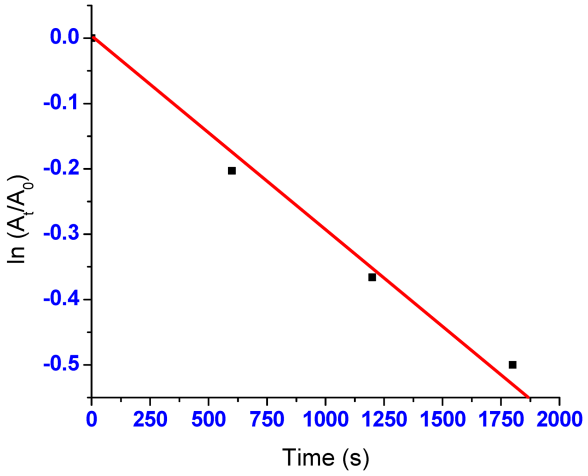

Fig. 7 *AuNPs catalysed reaction showing respective linear plots of ln (A_t/A_0) with time*

6 References

[1] Kelly, K.L., Coronado, E., Zhao, L.L., *et al.*: 'The optical properties of metal nanoparticles: The influence of size, shape, and dielectric environment', *J. Phys. Chem. B*, 2003, **107**, pp. 668–677

[2] Sau, T.K., Murphy, C.J.: 'Room temperature, high-yield synthesis of multiple shapes of gold nanoparticles in aqueous solution', *J. Am. Chem. Soc.*, 2004, **126**, pp. 8648–8649

[3] Pei, L.H., Mori, K., Adachi, M.: 'Formation process of two-dimensional networked gold nanowires by citrate reduction of $AuCl_4$− and the shape stabilization', *Langmuir*, 2004, **20**, pp. 7837–7843

[4] Tripathi, R.M., Shrivastav, A., Shrivastav, B.R.: 'Biofabrication of gold nanoparticles using leaf extract of Ficus benghalensis and their characterization', *Int. J. Pharma Biol. Sci.*, 2012, **3**, pp. 551–558

[5] Zhang, J., Zhao, B., Meng, L., *et al.*: 'Controlled synthesis of gold nanospheres and single crystals in hydrogel', *J. Nano Res.*, 2007, **9**, pp. 1167–1171

[6] Alekseeva, A.V., Bogatyrev, V.A., Khlebtsov, B.N., *et al.*: 'Gold nanorods: synthesis and optical properties', *Colloid J.*, 2006, **68**, pp. 661–678

[7] Hu, J.Q., Zhang, Y., Liu, B., *et al.*: 'Synthesis and properties of tadpole-shaped gold nanoparticles', *J. Am. Chem. Soc.*, 2006, **126**, pp. 9470–9471

[8] Chen, Y., Somsen, C., Milenkovic, S., *et al.*: 'Fabrication of single crystalline gold nanobelts', *J. Mater. Chem.*, 2009, **19**, pp. 924–927

[9] Iglesias, A.S., Grzelczak, M., González, B.R., *et al.*: 'Gold colloids with unconventional angled shapes', *Langmuir*, 2009, **25**, pp. 11431–11435

[10] Murphy, C.J., Gole, A.M., Hunyadi, S.E., *et al.*: 'One-dimensional colloidal gold and silver nanostructures', *J. Inorg. Chem.*, 2006, **45**, pp. 7544–7554

[11] Connor, E.E., Mwamuka, J., Gole, A., *et al.*: 'Gold nanoparticles are taken up by human cells but do not cause acute cytotoxicity', *Small*, 2005, **1**, pp. 325–327

[12] Jennings, T., Strouse, G.: 'Past, present, and future of gold nanoparticles', *Adv. Exp. Med. Biol.*, 2007, **620**, pp. 34–47

[13] Lee, Y., Lee, S.H., Kim, J.S., *et al.*: 'Controlled synthesis of PEI-coated gold nanoparticles using reductive catechol chemistry for siRNA delivery', *J. Control. Release*, 2011, **155**, pp. 3–10

[14] Daniel, M.C., Astruc, D.: 'Gold nanoparticles: assembly, supramolecular chemistry, quantum-size-related properties, and applications toward biology, catalysis, and nanotechnology', *Chem. Rev.*, 2004, **104**, pp. 293–346

[15] Sayed, I.H.E., Huang, X., Sayed, M.A.E.: 'Surface plasmon resonance scattering and absorption of anti-EGFR antibody conjugated gold nanoparticles in cancer diagnostics: applications in oral cancer', *Nano Lett.*, 2005, **5**, pp. 829–834

[16] Agarwal, M., Bhadwal, A.S., Kumar, N., *et al.*: 'Catalytic degradation of methylene blue by biosynthesized copper nanoflowers using F. benghalensis leaf extract', *IET Nanobiotechnol.*, 2016, **10**, pp. 321–325

[17] Tripathi, R.M., Shrivastav, A., Shrivastav, B.R.: 'Biogenic gold nanoparticles: As a potential candidate for brain tumor directed drug delivery', *Artif. Cells Nanomed. Biotechnol.*, 2015, **43**, pp. 311–317

[18] Tripathi, R.M., Kumar, N., Singh Bhadwal, A., *et al.*: 'Facile and rapid biomimetic approach for synthesis of HAp nanofibers and evaluation of their photocatalytic activity', *Mater. Lett.*, 2015, **140**, pp. 64–67

[19] Mehrotra, N., Tripathi, R.M., Zafar, F., *et al.*: 'Catalytic degradation of dichlorvos using biosynthesized zero valent iron nanoparticles', *IEEE Trans. Nanobiosci.*, 2017, **16**, pp. 280–286

[20] Tripathi, R.M., Rana, D., Shrivastav, A., *et al.*: 'Biogenic synthesis of silver nanoparticles using saraca indica leaf extract and evaluation of their antibacterial activity', *Nano Biomed. Eng.*, 2013, **5**, pp. 50–56

[21] Tripathi, R.M., Kumar, N., Shrivastav, A., *et al.*: 'Catalytic activity of biogenic silver nanoparticles synthesized by Ficus panda leaf extract', *J. Mol. Catal. B Enzym.*, 2013, **96**, pp. 75–80

[22] Mahajan, R., Bhadwal, A.S., Kumar, N., *et al.*: 'Green synthesis of highly stable carbon nanodots and their photocatalytic performance', *IET Nanobiotechnol.*, 2017, **11**, pp. 1–5

[23] Tripathi, R.M., Gupta, R.K., Bhadwal, A.S., *et al.*: 'Ultra-sensitive detection of mercury(II) ions in water sample using gold nanoparticles synthesized by

Trichoderma harzianum and their mechanistic approach', *Sens. Actuat. B*, 2014, **201**, pp. 637–646
[24] Tripathi, R.M., Gupta, R.K., Shrivastav, A., *et al.*: 'Trichoderma koningii assisted biogenic synthesis of silver nanoparticles and evaluation of their antibacterial activity', *Adv. Nat. Sci. Nanosci. Nanotechnol.*, 2013, **4**, pp. 035005–035010
[25] Tripathi, R.M., Gupta, R.K., Bhadwal, A.S., *et al.*: 'Fungal biomolecules assisted biosynthesis of Au–Ag alloy nanoparticles and evaluation of their catalytic property', *IET Nanobiotechnol.*, 2015, **9**, pp. 178–183
[26] Tripathi, R.M., Bhadwal, A.S., Singh, P., *et al.*: 'Mechanistic aspects of biogenic synthesis of CdS nanoparticles using Bacillus licheniformis', *Adv. Nat. Sci. Nanosci. Nanotechnol.*, 2014, **5**, (25006), p. 5
[27] Tripathi, R.M., Bhadwal, A.S., Shrivastav, B.R., *et al.*: 'ZnO nanoflower: Naovel biogenic synthesis and enhanced photocatalytic activity', *J. Photochem. Photobiol. B*, 2014, **141**, pp. 288–295
[28] Cohen, M.R., Smetzer, J.L.: 'Methylene blue is a monoamine oxidase inhibitor; severe harm and death associated with low-dose methotrexate; potentially dangerous mix-up between cancer drugs', *Hosp. Pharm.*, 2016, **51**, pp. 110–114
[29] Gillman, P.K.: 'Methylene blue implicated in potentially fatal serotonin toxicity', *Anaesthesia*, 2006, **61**, pp. 1013–1014
[30] Szpyrkowicz, L., Juzzolino, C., Kaul, S.N.: 'A comparative study on oxidation of disperse dyes by electrochemical process, ozone, hypochlorite and Fenton reagent', *Water Res.*, 2001, **35**, pp. 2129–2136
[31] Harrelkas, F., Azizi, A., Yaacoubi, A., *et al.*: 'Treatment of textile dye effluents using coagulation–flocculation coupled with membrane processes or adsorption on powdered activated carbon', *Desalination*, 2009, **235**, pp. 330–339
[32] Lu, X., Liu, L., Yang, B., *et al.*: 'Reuse of printing and dyeing wastewater in processes assessed by pilot-scale test using combined biological process and subfilter technology', *J. Clean Prod.*, 2009, **17**, pp. 111–114
[33] Aazam, E., Mohamed, R.: 'Environmental remediation of direct blue dye solutions by photocatalytic oxidation with cuprous oxide', *J. Alloys Compd.*, 2013, **577**, pp. 550–555
[34] Xu, M., Guo, J., Cen, Y., *et al.*: 'Shewanella decolorationis sp. nov., a dye-decolorizing bacterium isolated from activated sludge of a waste-water treatment plant', *Int. J. Syst. Evol. Microbiol.*, 2005, **55**, pp. 363–368
[35] Abadulla, E., Tzanov, T., Costa, S., *et al.*: 'Decolorization and detoxification of textile dyes with a laccase from Trameteshirsuta', *Appl. Environ. Microbiol.*, 2000, **66**, pp. 3357–3362
[36] Sakkayawong, N., Thiravetyan, P., Nakbanpote, W.: 'Adsorption mechanism of synthetic reactive dye wastewater by chitosan', *J. Colloid Interface Sci.*, 2005, **286**, pp. 36–42
[37] Gong, J.L., Wang, B., Zeng, G.M., *et al.*: 'Removal of cationic dyes from aqueous solution using magnetic multi-wall carbon nanotube nanocomposite as adsorbent', *J. Hazard. Mater.*, 2009, **164**, pp. 1517–1522
[38] Li, J., Zhu, J., Liu, X.: 'Ultrafine silver nanoparticles obtained from ethylene glycol at room temperature: catalyzed by tungstate ions', *Dalton Trans.*, 2014, **43**, pp. 132–137